Endochondral ossification is required for hematopoietic stem cell niche formation

Charles K. F. Chan[1,*], **Ching-Cheng Chen**[1,*], **Cynthia A. Luppen**[1,*], **Daniel L. Kraft**[1], **Jae-Beom Kim**[2,†], **Anthony DeBoer**[1], **Kevin Wei**[3], and **Irving L. Weissman**[1]

[1]Department of Pathology, Developmental Biology and Institute for Stem Cell Biology and Regenerative Medicine, Stanford University

[2]Department of Surgery, Division of Plastic and Reconstructive Surgery, Stanford University

[3]Department of Hematology, Stanford University

Abstract

Little is known about the formation of niches, local micro-environments required for stem cell maintenance. Here we develop an *in vivo* assay for adult hematopoietic stem cell (HSC) niche formation 1-2. With this assay, we identified a population of progenitor cells with surface markers $CD45^-Tie2^-\alpha_V^+CD105^+Thy1.1^-$ ($CD105^+Thy1^-$) that when sorted from 15.5 dpc fetal bones (fb) and transplanted under the adult mouse kidney capsule could recruit host-derived blood vessels, produce donor-derived ectopic bones through a cartilage intermediate, and generate a marrow cavity populated by host-derived long term reconstituting HSC (LT-HSC). In contrast, $CD45^-Tie2^-\alpha_V^+CD105^+Thy1^+$ ($CD105^+Thy1^+$) fb progenitors form bone that does not contain a marrow cavity. Suppressing expression of factors involved in endochondral ossification, such as osterix and VEGF, inhibited niche generation 22-24. $CD105^+Thy1^-$ progenitor populations derived from regions of the fetal mandible or calvaria that do not undergo endochondral ossification formed only bone without marrow in our assay27. Collectively, our data implicates endochondral ossification, bone formation that proceeds through a cartilage intermediate, as a requirement for adult HSC niche formation.

Growth and renewal in many tissues are initiated by stem cells, supported by the niches in which they reside1-3. While recent work has begun to describe functional interactions between stem cells and their niches, little is known about the formation of stem cell niches. Identification of the cells and processes that can generate, sustain and influence the HSC niche and hematopoiesis are critical for our understanding of normal hematopoiesis; stem cell homing, trafficking and differentiation; and hematopoietic pathology4-12. There is a need for modular systems in which the cellular and molecular components of a niche can be genetically modified and studied in an *in vivo* setting.

Correspondence and requests for materials should be addressed to C.C. (e-mail: chazchan@stanford.edu,) & C.C.C. (e-mail: c3chen@stanford.edu).

*These authors contributed equally to this work.
†Current address: Caliper Life Sciences, 2061 Challenger Dr., Alameda, CA 94501.

We have established an *in vivo* assay that permits functional assessment of the formation and maintenance of HSC niches at an ectopic site. We hypothesized that circulating HSC would colonize a non-hematopoietic location and establish functional hematopoiesis if appropriate niche components were present. We selected the subcapsular site of the kidney since it possesses a rich vascular supply, supports several kinds of tissue engraftment, and is not known to contain HSCs. In mice, HSCs are not detectable in the limb bone rudiment until 17.5 dpc[13]. In our initial experiments, we showed that transplantation of 14.5 dpc fetal bones (fb) under the kidney capsule, into either a GFP transgenic or CD45 congenic hosts, resulted in the formation of donor-derived bones with host-derived marrow and HSCs (Supplementary Fig. S2). This result indicates that 14.5 dpc fb contain elements that can initiate an ectopic niche. To determine if the fb must be intact for niche initiation, we dissociated the 14.5 dpc fb into a single cell suspension, embedded the suspension in matrigel, and introduced it under the kidney capsule. The suspension generated both cartilaginous and membranous bones that were populated with phenotypic and functional HSC (Fig. 1a – e, Supplementary Fig. S1a-b, S5). To distinguish donor from host tissue, we transplanted either fb from GFP transgenic mice or wild-type fb suspension transduced with lentiviral-GFP. The hematopoietic and vascular components within the ectopic niche were host-derived; non-hematopoietic and non-vascular components, including bone and cartilage were donor-derived (Supplementary Fig. S2, S3, S4). The engraftment and activity of host HSC within these ectopic niches has been verified by surface marker phenotype and functional long-term engraftment assays in secondary recipients (Supplementary Fig. S1a-b, Supplementary Fig. S5). We did not detect HSCs either in the ungrafted kidneys of transplanted mice, or in kidneys transplanted with matrigel only (Supplementary. Fig. S1a-b). To determine the kinetics of HSC colonization relative to ectopic bone formation, we evaluated both the presence of long-term HSCs (LT-HSC) and histological parameters of bone formation at 8-day intervals over a period of 32 days. Donor-derived bone was present at day 16 post transplant, coincident with the appearance of erythrocytes (Fig. 1e), and host-derived PECAM$^+$ vasculature. (Supplementary Fig. S3, S4). By day 24, c-kit$^+$ progenitors appeared; however, host-derived HSC were not detected until day 32. The day 32 grafts were structurally similar to normal bones with regions of cartilaginous, compact and trabecular bone (Fig. 1b - e). The presence of HSCs was found to be stable after the ectopic niche was established (data not shown).

To further characterize the progenitors responsible for bone formation and their role in hematopoietic niche formation and maintenance, we fractionated fb cell suspensions using a panel of cell surface markers for: putative mesenchymal stem cells (CD105 and Thy1.1), the angiopoietin receptor which is on a variety of hematopoietic and vascular cells (Tie2)[8], hematolymphoid cells (CD45), and a vascular integrin (α_V integrin)[14]. CD105 and Thy1.1 are also expressed on hematopoietic and endothelial cells but these cell types were negatively gated from the skeletal progenitors with CD45 and Tie2, respectively. By transplanting distinct donor fractions sorted by flow cytometry, we identified the minimal progenitor population required for the formation of a functional ectopic HSC niche. We found that CD105$^+$Thy1$^-$ progenitors consistently gave rise to bone with incorporated HSC-containing-marrow while equal numbers of CD105$^+$Thy1$^+$ progenitors resulted in bone formation without marrow (Fig. 2a-c, Supplementary Fig S1c). CD105-Thy- populations did

not form bones or niches efficiently. Thus far we have not observed marrow formation without bone, which suggests that bone forming cells such as osteoblasts, osteoblast progenitors, and/or osteoblast associated cells may be at least indirectly or structurally important for niche formation. It is important to note, however, that neither osteoblasts nor osteoblast progenitors alone were sufficient to initiate niche formation and HSC engraftment as the CD105^{+}Thy1^{+} population generated marrowless bone. To differentiate between the CD105^{+}Thy1^{-} bone and niche-generating and the CD105^{+}Thy1^{+} bone-generating populations, we conducted time course studies to compare the respective mechanisms of bone formation. We transplanted equal numbers of each population and harvested the grafted kidneys at 16 and 32 days post-transplantation for histological characterization. We found that only CD105^{+}Thy-1^{-} progenitors formed bones through a cartilage intermediate, also known as endochondral ossification, while CD105^{+}Thy1^{+} progenitors formed bones without a detectable cartilage intermediate (Figure 2b, c). Furthermore, we found that expression of osteocalcin, a marker of mature osteoblasts[15], was 5-fold higher in CD105^{+}Thy1^{+} populations derived from 15.5 dpc fb (Supplementary Fig. S1 d,e). These results suggest that CD105^{+}Thy1^{+} progenitors may have lost chondrocyte potential[16].

To assess the importance of specific candidate factors for niche development and HSC maintenance, we suppressed the expression of SLF, osterix and VEGF. SLF is essential for adult hematopoiesis and HSC activity[17], and is expressed by both mature osteoblasts[18] and endothelial cells[19]. We inhibited expression of SLF by transducing fb suspensions with a GFP-labelled, SLF-specific shRNA lentiviral vector prior to renal capsule transplant (Fig. 3d). We observed normal osteogenesis and niche formation when SLF expression was inhibited (Fig. 3 a, c). HSC engraftment was similar between mock-transduced and SLF-deficient grafts, consistent with our previous observation that SLF production is not essential for hematopoiesis during the fetal period[20]. To confirm the results of the knockdown, we transplanted intact 14.5 dpc fb from SLF null mutant (Sl/Sl) and again did not observe defects in either osteogenesis or niche formation (Fig. 3 b, c). This indicates that the SLF produced by skeletal progenitors and mature bone tissue is not required for initiation or maintenance of niche activity. We next silenced expression of osterix (Fig. 3e), a transcription factor necessary for endochondral ossification, in fb suspensions using lentivirus vector for osterix-specific shRNA[22,23]. The osterix knockdown severely inhibited osteogenesis and abolished niche formation, underscoring the dependence of niche formation on the process of endochondral ossification. Since perichondrial cells and chondrocytes in the developing limb express high levels of VEGF, and vascular invasion is critical to endochondral ossification[24], we tested whether VEGF activity was required for niche formation. We suppressed endogenous VEGF by injecting the host mice with adenovirus expressing soluble VEGF receptor (soluble Flk1; Ad-solVEGFR1), a known VEGF inhibiting reagent[25]. We found that endochondral ossification was disrupted when 13.5 dpc fb were transplanted into hosts treated with Ad-solVEGFR1 but not in hosts treated with control virus (Ad-Fc). The 13.5 dpc fb grafted into Ad-solVEGFR1 mice displayed an accumulation of chondrocytes without perfusing vasculature and marrow cavity although total HSC numbers in the host were not significantly affected (Fig. 3f)[26]. To further test the hypothesis that niche formation requires endochondral ossification, we isolated CD105+Thy- progenitors from the regions of fetal mandible and calvaria that form bone

primarily through intramembranous ossification27, which occurs without a cartilaginous intermediate. In these experiments CD105+Thy- mandibular and calvarial progenitors could only form marrowless bones even 60 days after transplantation (Fig. 4). These results suggest that endochondral ossification is necessary for niche formation.

A better functional understanding of the HSC niche was gained by observing how it is formed. In this study, CD105+Thy1.1- skeletal progenitors isolated from fetal limb bones initiated ectopic HSC niche formation. The progenitors gave rise to donor-derived chondrocytes, which recruited host-derived vasculature into the center of the developing bone graft. As endochondral ossification proceeded, the recruited vasculature facilitated the filling of the niche with host-derived hematopoietic cells: first erythroid and myeloid, then c-kit+ progenitors, and finally the HSCs. At this point we do not yet know if the CD105+Thy 1- cells represent a homogeneous population, or phenotypically similar but heterogeneous subsets. In agreement with our findings, Sacchetti et al recently identified CD146+ subendothelial cells residing in adult human bone marrow stroma that can generate both bone and marrow when transplanted under the skin of immunodeficient mice28. Although their study did not verify the presence of LT-HSC in the subdermal grafts, it is possible that osteoprogenitors in the adult marrow are involved in maintaining the niche. In addition to identifying the fetal bone derived skeletal progenitors that are capable of both endochondral ossification and HSC niche formation, our study provides a functional framework by which, in combination with previously described methods6,7, HSC-niche interactions can be further investigated at the cellular level.

Methods Summary

C57/BL6 CD45.1/2 congenic mouse strains were derived and maintained in our laboratory. Timed embryos from GFP transgenic HZ mice were used in the majority of the fetal bone (fb) transplantation studies. Sl/+ mice were purchased from Jackson laboratory.

Skeletal progenitors were isolated from fb (humerus, radius, tibia, femur, and pelvis, mandible without the condyle, and the individual frontal and parietal bones by collagenase digestion. They were next stained with antibodies against CD45, Tie2, α_V integrin, CD105 and Thy1.1 for fractionation by FACS. Sorted and unsorted skeletal progenitors were then injected underneath the renal capsule of 8-12 week old anesthetized mice.

SLF and osterix specific shRNA knockdown constructs, active lentiviral stock, and non-silencing shRNA constructs were generated as previously described (ref 29; supplementary table 1). Fb cell suspensions were transduced for 48hrs with specific shRNA vectors or control, sorted for GFP expression and transplanted as described.

To assess HSC engraftment in ectopic niches, grafted regions were dissected from kidney and crushed by mortar and pestle. Dissociated cells were stained with fluorochrome-conjugated antibodies against CD45, lineage (CD3, CD4, CD5, CD8, B220, Gr-1, Mac-1 and Ter119), c-Kit, Sca-1, and CD150 for FACS analysis. Sorted KLS, CD150+ LT-HSC were transplanted into lethally irradiated (800 rads delivered in split dose) by intravenous injection for functional analysis. Peripheral blood was obtained from the tail vein at 4 and 23 weeks after LT-HSC transplantation to assess donor-derived contributions by FACS.

Histological analyses of endochondral ossification were performed on sections that were obtained from either fresh frozen, OCT-embedded or formaldehye-fixed, paraffin-embedded specimens. Representative sections were stained with either Hematoxylin-and-Eosin, Movat's modified pentachrome[35], Safranin-O or Alizarin Red stains depending on the experiments.

RNA was extracted from sorted cells using Trizol (Invitrogen) or RNeasy RNA isolation kits (Qiagen) and was reverse-transcribed into cDNA with SuperscriptRT III (Invitrogen). SYBR Green Universal Master Mix and a GeneAmp 7000 or 7500 fast sequence detection system (Applied Biosystems) were used for real-time PCR with primers listed in supplementary table 2. Relative expression was calculated for each gene by the 2-   CT method with β-actin for normalization.

Supplementary Material

Refer to Web version on PubMed Central for supplementary material.

## Acknowledgments

References

1. Moore KA, Lemischka IR. Stem cells and their niches. Science (New York, N Y. 2006; 311(5769): 1880–1885.

2. Adams GB, Scadden DT. The hematopoietic stem cell in its place. Nature immunology. 2006; 7(4): 333–337. [PubMed: 16550195]

3. Wilson A, Trumpp A. Bone-marrow haematopoietic-stem-cell niches. Nature reviews. 2006; 6(2): 93–106.

4. Weissman IL. Normal and neoplastic stem cells. Novartis Foundation symposium. 2005; 265:35–50. discussion 50-34, 92-37. [PubMed: 16050249]

5. Kiel MJ, et al. SLAM family receptors distinguish hematopoietic stem and progenitor cells and reveal endothelial niches for stem cells. Cell. 2005; 121(7):1109–1121. [PubMed: 15989959]

6. Calvi LM, et al. Osteoblastic cells regulate the haematopoietic stem cell niche. Nature. 2003; 425(6960):841–846. [PubMed: 14574413]

7. Zhang J, et al. Identification of the haematopoietic stem cell niche and control of the niche size. Nature. 2003; 425(6960):836–841. [PubMed: 14574412]

8. Arai F, et al. Tie2/angiopoietin-1 signaling regulates hematopoietic stem cell quiescence in the bone marrow niche. Cell. 2004; 118(2):149–161. [PubMed: 15260986]

9. Wright DE, et al. Physiological migration of hematopoietic stem and progenitor cells. Science (New York, N Y. 2001; 294(5548):1933–1936.

10. Whitlock CA, Tidmarsh GF, Muller-Sieburg C, Weissman IL. Bone marrow stromal cell lines with lymphopoietic activity express high levels of a pre-B neoplasia-associated molecule. Cell. 1987; 48(6):1009–1021. [PubMed: 3493849]

11. Moore KA, Ema H, Lemischka IR. In vitro maintenance of highly purified, transplantable hematopoietic stem cells. Blood. 1997; 89(12):4337–4347. [PubMed: 9192756]

12. Dexter TM, Allen TD, Lajtha LG. Conditions controlling the proliferation of haemopoietic stem cells in vitro. Journal of cellular physiology. 1977; 91(3):335–344. [PubMed: 301143]

13. Christensen JL, Wright DE, Wagers AJ, Weissman IL. Circulation and chemotaxis of fetal hematopoietic stem cells. PLoS biology. 2004; 2(3):E75. [PubMed: 15024423]

14. Cheresh DA. Human endothelial cells synthesize and express an Arg-Gly-Asp-directed adhesion receptor involved in attachment to fibrinogen and von Willebrand factor. Proceedings of the National Academy of Sciences of the United States of America. 1987; 84(18):6471–6475. [PubMed: 2442758]

15. Geoffroy V, Ducy P, Karsenty G. A PEBP2 alpha/AML-1-related factor increases osteocalcin promoter activity through its binding to an osteoblast-specific cis-acting element. The Journal of biological chemistry. 1995; 270(52):30973–30979. [PubMed: 8537354]

16. Akiyama H, et al. Osteo-chondroprogenitor cells are derived from Sox9 expressing precursors. Proceedings of the National Academy of Sciences of the United States of America. 2005; 102(41): 14665–14670. [PubMed: 16203988]

17. Fleischman RA, Mintz B. Prevention of genetic anemias in mice by microinjection of normal hematopoietic stem cells into the fetal placenta. Proceedings of the National Academy of Sciences of the United States of America. 1979; 76(11):5736–5740. [PubMed: 42904]

18. Blair HC, et al. Parathyroid hormone-regulated production of stem cell factor in human osteoblasts and osteoblast-like cells. Biochemical and biophysical research communications. 1999; 255(3): 778–784. [PubMed: 10049787]

19. Aye MT, et al. Expression of stem cell factor and c-kit mRNA in cultured endothelial cells, monocytes and cloned human bone marrow stromal cells (CFU-RF). Experimental hematology. 1992; 20(4):523–527. [PubMed: 1373691]

20. Ikuta K, Weissman IL. Evidence that hematopoietic stem cells express mouse c-kit but do not depend on steel factor for their generation. Proc Natl Acad Sci U S A. 1992 Feb 15; 89(4):1502–6. [PubMed: 1371359]

21. Heissig B, et al. Recruitment of stem and progenitor cells from the bone marrow niche requires MMP-9 mediated release of kit-ligand. Cell. 2002; 109(5):625–637. [PubMed: 12062105]

22. Nakashima K, et al. The novel zinc finger-containing transcription factor osterix is required for osteoblast differentiation and bone formation. Cell. 2002; 108(1):17–29. [PubMed: 11792318]

23. Koga T, et al. NFAT and Osterix cooperatively regulate bone formation. Nature medicine. 2005; 11(8):880–885.

24. Zelzer E, et al. VEGFA is necessary for chondrocyte survival during bone development. Development (Cambridge, England). 2004; 131(9):2161–2171.

25. Jacobi J, et al. Adenoviral gene transfer with soluble vascular endothelial growth factor receptors impairs angiogenesis and perfusion in a murine model of hindlimb ischemia. Circulation. 2004; 110(16):2424–2429. [PubMed: 15477417]

26. Maes C, et al. Impaired angiogenesis and endochondral bone formation in mice lacking the vascular endothelial growth factor isoforms VEGF164 and VEGF188. Mechanisms of development. 2002; 111(1-2):61–73. [PubMed: 11804779]

27. Hall BK, Miyake T. All for one and one for all: condensations and the initiation of skeletal development. Bioessays. 2000; 22(2):138–147. [PubMed: 10655033]

28. Sacchetti B, et al. Self-renewing osteoprogenitors in bone marrow sinusoids can organize a hematopoietic microenvironment. Cell. 2007; 131(2):324–336. [PubMed: 17956733]

29. Metz M, et al. Mast cells can enhance resistance to snake and honeybee venoms. Science (New York, N Y. 2006; 313(5786):526–530.

30. Garvey W, et al. Improved Movat pentachrome stain. Stain technology. 1986; 61(1):60–62. [PubMed: 2420041]
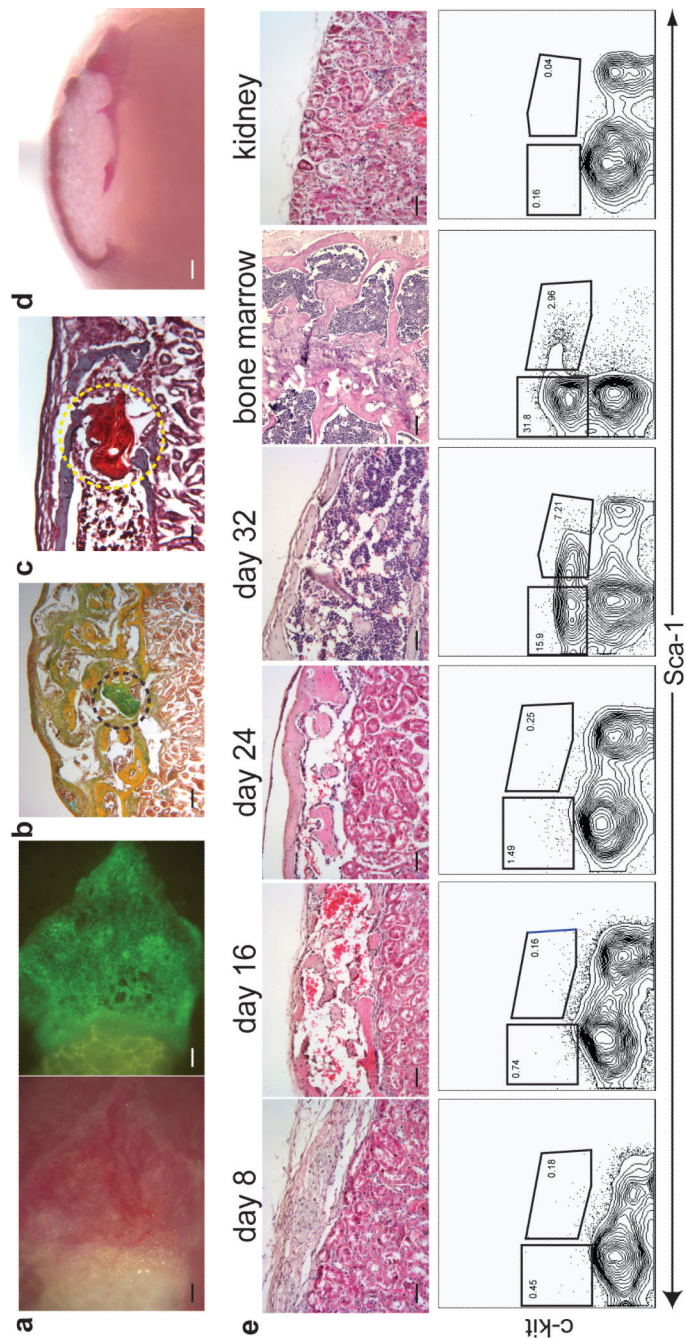
Figure 1.

Fetal bone (fb) cells can initiate an ectopic HSC niche. **a**, Ectopic bone formed by GFP-labelled, 14.5 dpc fb cells 32 days after subrenal capsule transplant (scale bar = 500 μM). **b**, Representative section of graft stained with pentachrome (yellow=osteoid, greenish blue= cartilage), cartilaginous region in black circle (scale bar = 100 μM). **c**, Safranin-O stain of adjacent section, red-staining cartilage matrix in yellow circle (scale bar = 200 μM). **d**, Alizarin Red stain for calcified tissue (scale bar = 500 μM). **e**, Time course study of hematopoietic components during ectopic niche formation. Hematoxylin-and-Eosin staining

(upper panel, scale bar = 100 μM), representative FACS profiles of LT-HSC (CD45$^+$Lineage$^-$c-Kit$^+$Sca1$^+$CD150$^+$) frequency that were pre-gated for live, CD45$^+$lineage$^-$ cells (lower panel). Days after transplantation are indicated; (n=4) for each time point.
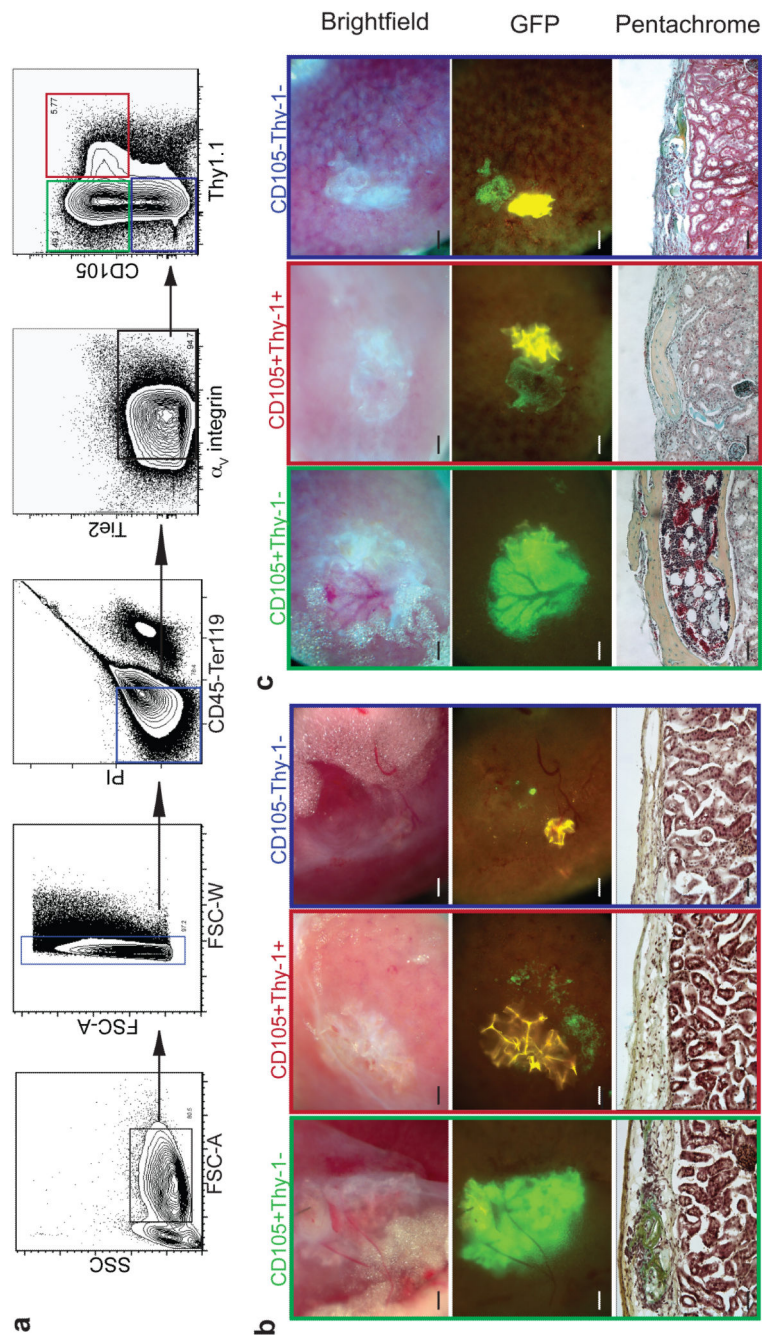
Figure 2.
CD105+Thy-1- population forms ectopic HSC niche through a cartilaginous intermediate. **a**, Representative FACS profile of homogenized 15.5 dpc fb pre-gated for live CD45-Ter119- cells showing CD105+Thy-1-, CD105+Thy-1+, and CD105-Thy-1- populations (green, red and blue gates, respectively). **b-c**, 2000 double-sorted fb cells from each fraction were injected under renal capsule and harvested 16 days (n=4) (b) or 32 days (n=13) (c) after transplantation. Brightfield (upper panel) and GFP images (middle panel) of explanted
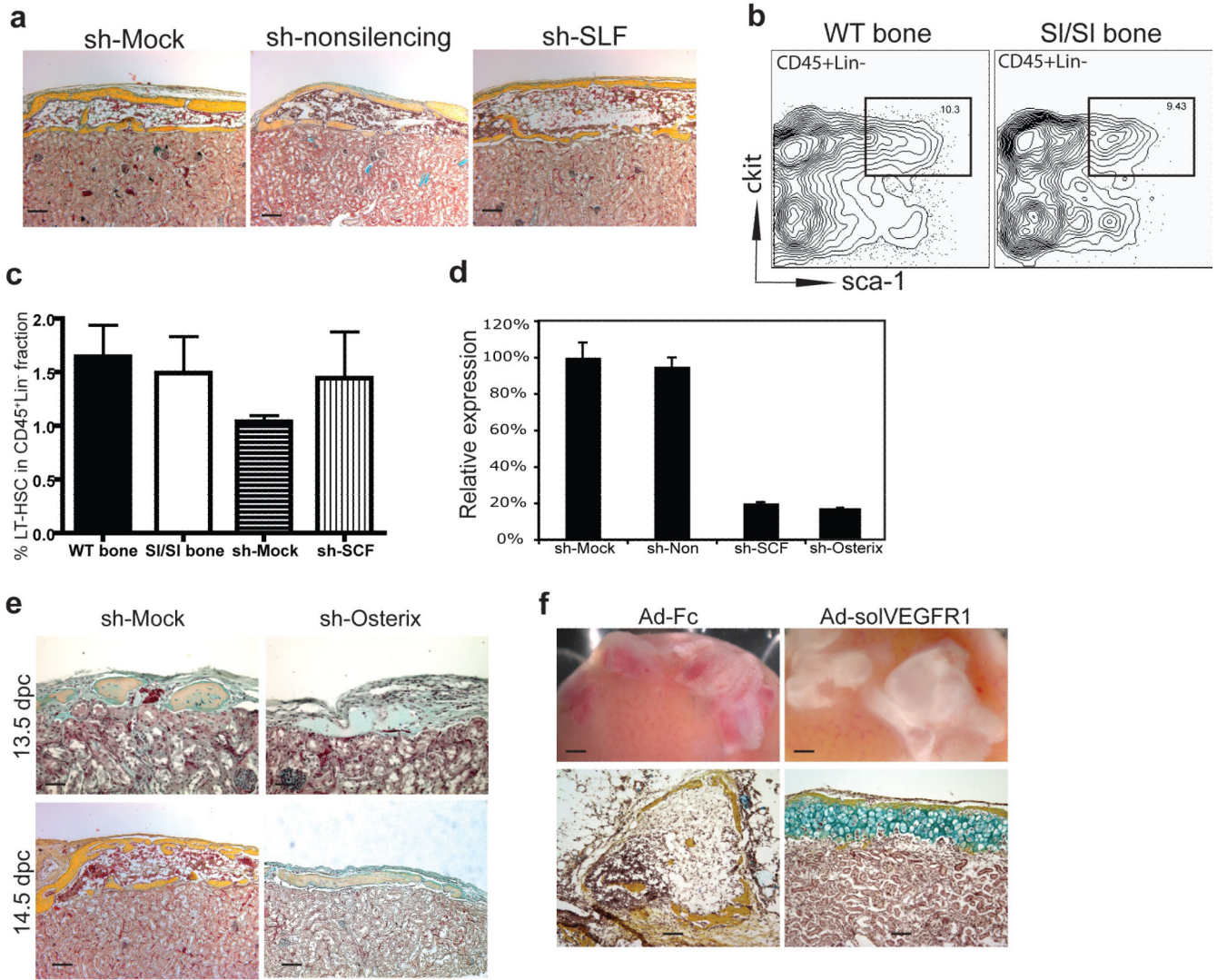
ectopic grafts. Pentachrome staining of transverse sections through grafts at 16 and 32 days (lower panel). (Scale bar in upper and middle panels = 500 μM, in lower panel = 100 μM).
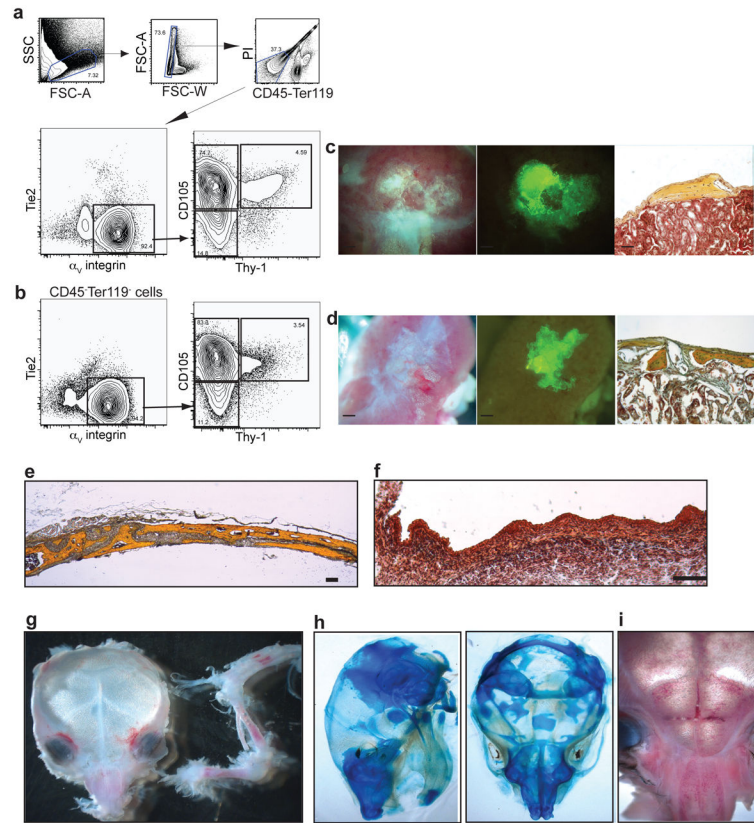
Figure 3.
Niche formation is dependent on endochondral ossification. **a-c**, Suppression of SLF expression in fb cells did not alter osteogenesis or niche formation. 14.5 dpc fb cells were transduced with lentivirus as indicated, and 2000 sorted GFP+ cells were injected under the renal capsule. **a**, Paraffin-embedded sections were obtained 32 days after transplantation and stained with pentachrome. **b**, Representative FACS profiles of pre-gated, live CD45^{+}lineage^{-} cells harvested from intact 15.5 dpc normal (WT) or mutant (Sl/Sl) fetal bones 40 days after transplantation (n=4). **c**, Frequency of LT-HSC in different ectopic niches shown in mean values ± Standard error of the mean (SEM) (WT bone n=3, Sl/Sl bone n=4, sh-Mock n=6, sh-SLF n=3). **d**, Knockdown efficiency of sh-SLF and sh-Osterix was determined by qRT-PCR in 1A5 osteoblast cell line. Relative expression percentage shown in mean values ± Standard Deviation (SD) (n=3). **e**, Suppression of osterix expression disrupted osteogenesis and niche formation. Fetal bone cells from 13.5 dpc (upper panel) or 14.5 dpc (lower panel) were transduced with the lentivirus indicated and 2,000 sorted GFP+ cells were transplanted (n=4). **f**, VEGF is required for formation of bone marrow cavity. Adult C57Bl/6 mice were

intravenously injected with 10^8 m.o.i of the adenovirus constructs expressing either mouse Fc (Ad-Fc) or soluble ectodomain of VEGFR1 (Ad-solVEGFR1) (n=3). Two days after virus injection, 13.5 dpc fb elements were transplanted under the renal capsule. Paraffin-embedded sections were obtained 25 days after transplantation and stained with pentachrome. (Scale bars in brightfield images = 500 μM, in pentachrome-stained images = 100 μM).

Figure 4.
Skeletal progenitors from mandible and calvaria do not form HSC niches efficiently. **a-b**, Representative FACS profile of homogenized 15.5 dpc mandible (n=6) (a) or calvaria (n=6) (b) pre-gated on live CD45⁻Ter119⁻ cells. 2000 sorted GFP⁺ CD105⁺Thy-1⁻. **c-d**, Cells from mandible (c) or calvaria (d) were transplanted under renal capsule and harvested after 32 days. **e**, Pentachrome stained cross section of mouse parietal bone at 4 weeks. **f**, Pentachrome stained cross section of equivalent area in e15 dpc fetal calvaria. **g-i**, Marrow pockets in calvaria are concentrated in facial areas corresponding to cartilaginous regions (n=3). Limb bones are juxtaposed to skull for comparison. **h**, Dorsal and lateral views of newborn calvaria show cartilaginous regions that stain with alcian blue. (Scale bar in brightfield and GFP images = 500 μm, in pentachrome images = 100 μm, in (f) =25 μm).